

Designing Groundless Body Channel Communication Systems: Performance and Implications

Virag Varga
ETH Zurich & Disney Research
Zurich, Switzerland

Marc Wyss
ETH Zurich
Zurich, Switzerland

Gergely Vukulya
ETH Zurich & Disney Research
Zurich, Switzerland

Alanson Sample
Disney Research
Los Angeles, CA, USA

Thomas R. Gross
ETH Zurich
Zurich, Switzerland

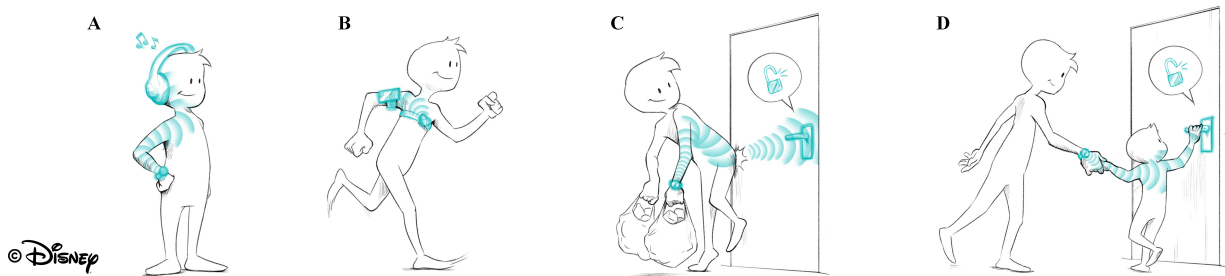


Figure 1. Illustration of novel interactions and connectivity options using Body Channel Communication. (A) Streaming music from a smartwatch through the body to the headphones; (B) Forming on-body sensor network between smartphones and heart rate monitor chest bands; (C) Authenticating and unlocking smart doors with elbows or hips; (D) Parental control to enable children opening doors only in the presence of adults.

ABSTRACT

Novel interactions that capacitively couple electromagnetic (EM) fields between devices and the human body are gaining more attention in the human-computer interaction community. One class of these techniques is Body Channel Communication (BCC), a method that overlays physical touch with digital information. Despite the number of published capacitive sensing and communication prototypes, there exists no guideline on how to design such hardware or what are the application limitations and possibilities. Specifically, wearable (*groundless*) BCC has been proven in the past to be extremely challenging to implement. Additionally, the exact behavior of the human body as an EM-field medium is still not fully understood today. Consequently, the application domain of BCC technology could not be fully explored. This paper addresses this problem. Based on a recently published general purpose wearable BCC system, we first present a thorough evaluation of the impact of various technical parameter choices and an exhaustive channel characterization of the human body as a host for BCC. Second, we discuss the implications of these

results for the application design space and present guidelines for future wearable BCC systems and their applications. Third, we point out an important observation of the measurements, namely that BCC can employ the whole body as user interface (and not just hands or feet). We sketch several applications with these novel interaction modalities.

CCS Concepts

•**Human-centered computing** → *Empirical studies in ubiquitous and mobile computing; Interaction techniques;*

Author Keywords

body channel communication; capacitive coupling; channel characterization; empirical study; wearables; guideline; interaction techniques

INTRODUCTION

Systems that actively generate electromagnetic fields and use capacitive coupling to let electric signals propagate through the human body have been explored in various human-computer interaction projects, either for digital communication [5, 10, 42] or active sensing [6, 29, 43]. In just the last few years, example uses have included augmented clothes and fabric [8, 27, 32], human body augmentation [17, 18, 36, 41], touch and gesture recognition [17, 21, 32], grip and grasp recognition [40], whole-body movement recognition [12], indoor localization [12], shape sensing [15], user identification and personalization of devices and interfaces [14, 16, 35], games and playful interactions [33], and general purpose touch-controlled

Permission to make digital or hard copies of all or part of this work for personal or classroom use is granted without fee provided that copies are not made or distributed for profit or commercial advantage and that copies bear this notice and the full citation on the first page. Copyrights for components of this work owned by others than the author(s) must be honored. Abstracting with credit is permitted. To copy otherwise, to republish, to post on servers or to redistribute to lists, requires prior specific permission and/or a fee. Request permissions from permissions@acm.org.

UIST '18, October 14–17, 2018, Berlin, Germany

© 2018 Copyright held by the owner/author(s). Publication rights licensed to ACM. ISBN 978-1-4503-5948-1/18/10...\$15.00

DOI: <https://doi.org/10.1145/3242587.3242622>

data transfer [34, 39]. Behind this broad range of applications and research directions there exist a number of independent hardware prototype designs with individual parameters. The choice of transmission frequency illustrates well the diversity of Body Channel Communication (BCC): while the official standard on BCC [2] locks the center frequency at 21 MHz, most of the implemented systems use either much lower or higher frequencies: a few tens or hundreds kHz [7, 10, 16, 26, 29, 35, 39, 42], around 1-10 MHz [13, 24, 29, 33, 34], or even 80 MHz [41].

In fact, the frequency is one of the most important parameters that set BCC systems apart, because usually it dictates the limitations in scalability, robustness, achievable physical range, portability, and/or data rate. When the frequency drops lower than approx. 1 MHz, the electric field transmission without direct ground connection becomes very sensitive to noise. Wearable systems without this explicit ground connection (informally: *groundless systems*) usually cannot function in this range or just with severe limitations like minimal transmission path or special installation environments. On the other hand, higher frequencies result in stronger signals with the cost of increasing the effect of over-the-air coupling as well. Such a design can lead to situations when proximity of several meters triggers false positive touch-events. Wearable systems that intend to keep the actual touch-trigger characteristic usually must limit their carrier frequency, typically resulting in the frequency range of 2-10 MHz. The challenge of designing wearable BCC systems and applications is to find the optimal configurations (including but not limited to the exact frequency in this 2-10 MHz range) that balance the (preferably high) signal strength with (preferably low) over-the-air coupling.

The other important aspect of capacitively coupled systems is that as by today the physical phenomenon behind the concept – namely how exactly the human medium behaves when exposed to electric fields – is still not fully understood. The lack of complete characterization of the human medium also prevents establishing widely accepted guidelines for wearable BCC system design or applications.

This paper aims to fill this void. We use a recently published stand-alone, end-to-end, wearable BCC system [34], and we measure the signal strength throughout the whole body in several configurations. This setup allows to draw conclusions on how an actual system may perform across varying parameters of the device, the user, and/or the environment. Based on the measurements this paper presents three contributions:

- (i) This paper is the first comprehensive quantified study that charts the EM-field carrying property of the human body in detail.
- (ii) We provide design guidelines for future BCC systems which connect the physical phenomena and the technical aspects with the application designer’s perspective to provide recommendations on various design parameters (size, configuration, and distance of the electrodes) and usability options (device placement, body position, movements, detailed hand heatmaps), while we also vali-

date the robustness of the technology (across time, space, users).

- (iii) We expose new capabilities and interactions with BCC. The results show that BCC wearables can operate at arbitrary body positions – not just at limbs – to perform as on-body sensors. Also, regardless of the devices’ placement, the whole body (any part of it) can participate in interactions. Moreover, we explore what two-people-BCC-interactions may do. These observations trigger ideas for new placement options (head-mounted device, necklace, belt, pocket, leg attachments) and can also introduce novel interactions (with shoulders, elbows, hips, knees) or complexities (chain of people).

RELATED WORK

In the past, a couple of experimental and some theoretical studies have attempted to establish a common understanding on how the human body behaves while it is being exposed to electric signals and fields. Most of these studies swipe through a wide range of frequencies (typically in the 100 kHz-200 MHz range) to understand how the propagation in and around the body is dependent on the choice of the carrier frequency. To set up such testbed systems, usually heavy instruments are used to generate and receive signals, such as signal generators [31], oscilloscopes [31], spectrum analyzers [4], or network analyzers [22, 23]. As explained later in Section *Design of the Experiment Setup*, BCC devices are very sensitive to any attached additional conductors (including measuring instruments): by adding new elements to the system we risk changing the signal that we intend to observe. Therefore, systems tend to use so called *balun transformers* when they connect the extra (usually earth-grounded) instruments to the transmitter (TX) or receiver (RX). However, we argue that even though these balun transformers indeed prevent a direct connection to the earth ground, some parasitic signals can still flow through, preventing BCC systems to be truly evaluated as wearables. On the other hand, measurement setups that use wave generators as TX (i.e., they use single frequency, unmodulated sine waves) [4, 22, 23, 25, 28, 30, 31] are not designed for arbitrary data transfer, and therefore do not allow an accurate assessment of the behavior during BCC traffic. Moreover, these systems focus mostly on the changing carrier frequency and do not necessarily analyze all parameters at a level that would be interesting for a wearable BCC system.

There exist only a few channel characterization studies that use real wearable BCC devices for evaluation with actual modulated signals. [38] uses a wearable TX-RX pair, and focuses on the 1 MHz to 1 GHz frequency domain. While several interesting effects are investigated, like interference from nearby users and objects, only 3 different body locations are covered. Effects of electrode placement are analyzed through simulations. No user specific parameters are measured, nor is temporal stability verified. The other system that uses modulated data in a wearable setup is [26]. 3 locations are reported with the RX coming in 3 form factors (shoe, belt, watch), while the TX is lying on a desk. Notes mention other parameters like electrode size, hand- and footwear, but no data is shown.

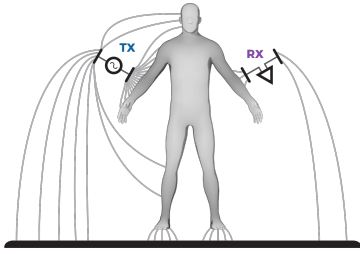


Figure 2. The quasi-static field surrounding the human body is originating from the several capacitances that occur between all combinations of the transmitter, the receiver, the human, and the earth ground.

Besides the experimental approaches, there have been a few attempts to approach BCC from theoretical point of view by defining approximate electromagnetic models. Some previously mentioned papers also presented theoretical models [4, 38]. Additionally, a series of simulation data is shown in [19] as well.

DESIGN OF THE EXPERIMENT SETUP

Body Channel Communication can be implemented in several, fundamentally different, ways. This paper focuses on a system that capacitively couples electric fields on the body. In the corresponding electric model the body is described as one node of the electric circuit [42], while the dominant phenomenon is a quasi-static electric field around it [4] (see Figure 2).

The circuit between TX and RX is on one end closed by the user's body, while on the other end by a common ground. Considering that in our case the TX and RX devices are mostly wearables, the common ground is usually established through parasitic capacitive air-coupling towards the earth ground (therefore wearables can be informally be referred to as *groundless* or more precisely *floating ground devices*). Any electrical device or plain conductor attached to the TX or RX changes their grounding property since capacitances are dependent on plate size, and so these increased capacitances towards the common (earth) ground would result in stronger signals.

The quasi-static property ensures that the signal (as a series of varying high and low voltage states) changes the same way (direction, frequency, phase) throughout the field, e.g., the human body. However, since - amongst others - the capacitances (that are also dependent on the distance) towards the ground are different at different body locations, different RX placements on the body would result in different signal strength. In other words: BCC does not guarantee the same signal strength throughout (of positions of) the body. Hence, the human body, as the channel of a communication system that is based on electric fields, is not a homogeneous medium.

To design future applications that utilize BCC, we need to get a more detailed understanding of how the body channel behaves and what performance can be achieved. Therefore, we built a testbed to measure the signal strength under different circumstances at different points of the body.

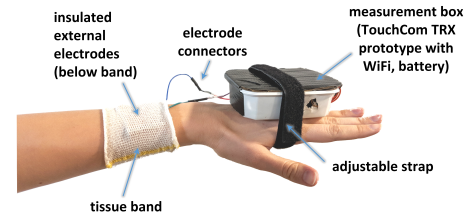


Figure 3. To ensure reproducibility, the BCC device is attached to the body in a controlled way. A small plastic box holds the board and battery. The electrodes are interchangeable, and they are tied to the body by a thin tissue band to allow flexibility with the electrode placement. The electrode themselves are insulated, having a piece of copper tape inside.

Since (as explained above) capacitively coupled BCC systems are sensitive to additional equipment as it would change their grounding capability, the testbed is set up in such a way that it observes a portable BCC communication system under real working conditions without interfering with the system's performance, and it presents signal strength values calculated from this real data traffic.

TouchCom prototype platform

The TouchCom prototype platform is a recently presented [34], general purpose BCC hardware-software system, which provides bidirectional communication between BCC endpoints, and which among others supports wearable designs as well. The advantage of TouchCom is the central role of software control: most aspects can be easily changed by modifying software parameters, e.g., the carrier frequency. This architecture allows great flexibility and easy customization, making TouchCom suitable to build a testbed around it. The implemented communication stack uses on-off keying modulation as physical layer, with a 21.875 kHz baseband control signal. The carrier frequency can be freely selected by the software in the range of 1 to 10 MHz. As a consequence of the simple and robust design of TouchCom, the TRX has some non-linear properties that also reflect on the peak-to-peak output voltage: for frequencies of 2, 3, 4, and 8 MHz the V_{pp} is 5.9, 8.6, 9.9, and 6.1 V, respectively. The TouchCom boards need 8-12 V input voltage for operation, which can be supplied from a single battery, achieving galvanic separation from the earth ground.

Hardware and software testbed design

While the environment (indoors/outdoors/heavily equipped) could also influence the performance, the signal strength might be affected by the user him- or herself as well (body type, hydration level, etc.). To ensure that the measurements are conducted under the same conditions, a device with a special form factor is built (Figure 3), which can be easily attached to the arms, legs, or waist by an adjustable length strap. Since several properties of the applied electrodes are evaluated, instead of using fixed electrodes, connectors are added to the TouchCom board that make it possible to easily attach any electrode during the measurements. Figure 4 depicts the primary locations we consider for BCC device placement, while the user is in the standard standing position.

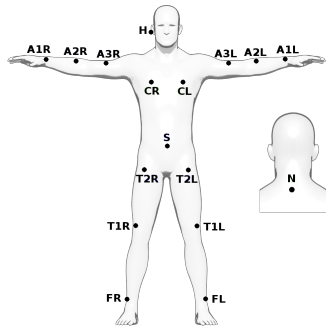


Figure 4. Standard standing position. The arms are wide spread apart, in a 90 degree angle from the body. The points indicate possible placements of BCC devices.

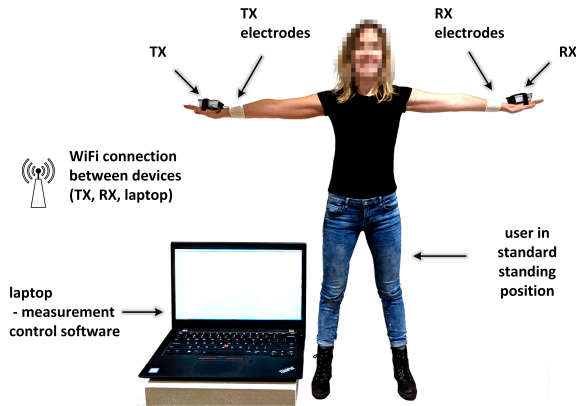


Figure 5. Typical measurement setup using A1R and A1L device placement locations. The TX and RX devices are battery powered and connect to the laptop via WiFi. This setup ensures that there is no extra instrumentation.

Additional WiFi chips may be connected to the TouchCom boards allowing convenient experiment control and facilitated data collection. This backbone system does not affect the BCC transmission (it operates in the gigahertz domain) but makes it possible to easily access and integrate the TouchCom prototypes into an automated measurement system. The testbed setup is shown in Figure 5.

After the transceivers (TRX) are placed and attached to the desired position, a semi-automated desktop program wirelessly triggers a continuous transmission from the transmitter (TX) side, while the other TRX starts to operate as receiver (RX) for in-depth data collection. The TX keeps sending 13-byte long packets every 10 ms, with a payload that has a sufficient number of on and off symbols to allow enough data to approximate the average high and low voltage levels. Due to memory limitations of the microcontroller, the RX log period lasts only for approx. 300 ms¹. The recorded values are kept in the memory of the RX until they are explicitly downloaded to the processing computer. This operation ensures that the measurement process does not interfere with the incoming signal –

¹The dedicated RX buffer size is 64 kB. Using 12-bit precision, 32768 ADC values (2 B) can be stored. The sample rate is set to five times oversampling of the baseband frequency ($5 * 21.875 \text{ kHz} = 109.375 \text{ kHz}$). Therefore, the maximum duration of a loggable period is $32768 / 109.375 \text{ kHz} = 299.6 \text{ ms}$.

no downlink stream is established, nor are any extra devices attached to the RX during the transmission period. When the logging period has finished, the measurement program automatically downloads the recorded data, then it repeats the whole procedure – with a short break – two more times. In total, approx. 1 s measurement data is recorded for each setup.

Metric

Throughout the upcoming sections, we present SNR (signal-to-noise ratio) values as comparable indicators of the signal strength in different setups. (For a complete discussion of the relationship between measured SNR values and actual network performance, see Subsection *Interpreting signal-to-noise ratio values* in the discussion section.) The TouchCom prototype platform gives the following equation on how to translate the traditional $SNR = 10 \times \log_{10} \frac{P_{signal}}{P_{noise}}$ formula (with P_{signal} the power of the signal, and P_{noise} the power of background noise) into one that uses only the already digitized incoming signal values:

$$SNR = 7.304 \cdot \ln \left(\frac{ADC_H - 380.612}{ADC_L - 380.612} \right) [dB]$$

where ADC_H and ADC_L are the corresponding average ADC values for the input voltage of every received high and low values of the modulated packets [34]. To ensure that even very weak incoming signals can be measured properly (when the intervals of low and high values start to merge together), we define ADC_H as the rightmost (high) peak in the distribution of all recorded ADC values in session, and ADC_L as the leftmost (low) peak.

Safety

The TouchCom system follows the *ICNIRP* guidelines [1] that define regulations on the current density and on SAR (specific energy absorption rate).² The maximum contact current of one TouchCom device is less than 0.5 mA subject to the safety limit of 20 mA; the whole-body average SAR is less than 1 mW/kg subject to the safety limit of 80 mW/kg. When multiple devices are in use, their effects are additive, resulting in the limit of 40 simultaneous devices per person.

MEASUREMENT RESULTS

The measurements presented here consider several body positions, locations, and users, as well as several technical parameters of the BCC device. If not explicitly stated otherwise, the measurements are performed with A1R-A1L coupler locations, with a dedicated user (subject #6), in the standard standing position (see Figure 4 and Table 11 for details). In this body position the devices are placed at the maximal distance from each other and from the earth ground, resulting in the least favorable conditions for signal propagation during the BCC transmission due to the longer distance, to the reduced possibility for extra (unwanted) air-coupled signals, and to the weak ground connection. The electrodes in use are insulated copper plates, with the default size of $4 \times 4 \text{ cm}^2$ for the signal and $4 \times 6 \text{ cm}^2$ for the ground electrodes.

²The current density is limited to prevent effects on nervous system functions, while the SAR limitation ensures avoidance of whole-body heat stress and excessive localized tissue heating.

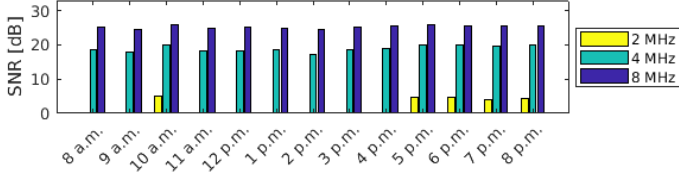


Figure 6. Measurements taken throughout a day for three different frequencies (2, 4, 8 MHz). The mean and standard deviation of each frequency: $SNR_{2MHz} = 1.77$ dB (with $SD=2.34$); $SNR_{4MHz} = 18.92$ dB (with $SD=0.94$); $SNR_{8MHz} = 25.22$ dB (with $SD=0.43$).

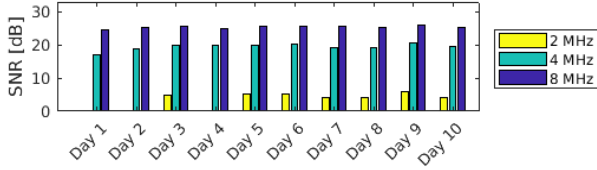


Figure 7. Measurements taken throughout ten consecutive days for three different frequencies (2, 4, 8 MHz). The mean and standard deviation of each frequency: $SNR_{2MHz} = 3.37$ dB (with $SD=2.39$); $SNR_{4MHz} = 19.42$ dB (with $SD=1.04$); $SNR_{8MHz} = 25.38$ dB (with $SD=0.40$).

Reproducibility

EM-field based communication systems tend to be sensitive to changes in the environment, to device placements, to the user itself, etc. To ensure that our measurement method gives reproducible results, a series of temporal, spatial, and user-specific measurements are performed.

Figure 6 shows the measured signal strength throughout a day, while Figure 7 shows measurements taken on several consecutive days. On the 2 MHz carrier frequency, the signal tends to be weak – on several occasions the signal merges with the noise floor, resulting in 0 dB SNR. On 4 MHz and 8 MHz, the performance can be considered strong and stable: the standard deviation is below 1.04 between the measurements taken at different times.

The aim of this paper is to understand how BCC can be set up for wide range of uses as an everyday technology. Hence the performance should be validated in different environments. Figure 8 shows minimal variations of the signal strength (standard deviation 0.4) across work, living, and outdoors environments.

The third important variable is the user himself/herself. The clothing and footwear may have an impact on the electric fields, however, their impact does not seem to be significant.

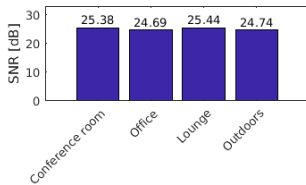


Figure 8. Transmission measured at various locations. The office setup has the most EM-noise from nearby equipment and numerous wireless devices. The average $SNR = 25.06$ dB (with $SD=0.40$). The carrier frequency is set to 8 MHz.

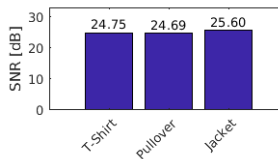


Figure 9. Transmission measured with different clothing. The average $SNR = 24.89$ dB (with $SD=0.23$). The carrier frequency is set to 8 MHz.

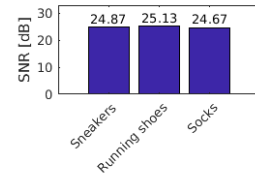


Figure 10. Transmission measured with different footwear. The average $SNR = 25.01$ dB (with $SD=0.51$). The carrier frequency is set to 8 MHz.

While Figure 9 plots the effects of different clothing, Figure 10 investigates the effect of different footwear. In both cases every other parameter is fixed (same user, same environment, same technical parameters for BCC device).

Subject	Gender	Age	Height	Weight	Footwear
#1	male	59 years	178 cm	70 kg	slippers
#2	female	55 years	164 cm	65 kg	slippers
#3	female	19 years	175 cm	63 kg	barefoot
#4	female	21 years	167 cm	65 kg	5-finger shoes
#5	female	29 years	169 cm	53 kg	sneakers
#6	male	23 years	178 cm	80 kg	sneakers
#7	male	23 years	174 cm	68 kg	running shoes
#8	male	23 years	190 cm	85 kg	sneakers

Figure 11. Pool of participants. Most of the measurements are performed by subject #6.

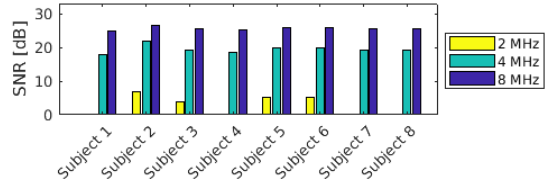


Figure 12. Measurements with several users in freely chosen body position. Three different frequencies are measured: 2, 4, 8 MHz. The mean signal strength and standard deviation for each frequency: $SNR_{2MHz} = 2.61$ dB (with $SD=2.89$); $SNR_{4MHz} = 19.50$ dB (with $SD=1.21$); $SNR_{8MHz} = 25.59$ dB (with $SD=0.48$).

A set of measurements are also taken to validate that the system performs similarly across different users. Figure 12 shows that even though there is variation in the signal strength among different users (pool of participants is described in Figure 11), it is not significant.

Therefore, we conclude that our setup is reproducible, and we proceed presenting measurements taken by one user, in one location, with a set of dedicated clothing and footwear. This approach ensures that as many parameters are fixed throughout the measurement campaign as possible.

Physical Design Parameters of BCC Devices

To design optimal BCC end user devices, the relationship between physical characteristics and the resulting signal strength must be understood. We present the most important design parameters (ground electrode size, signal electrode size, wire length, in between materials, electrode distance) and their impact on Figures 13-18. All of these measurements are collected on 8 MHz.

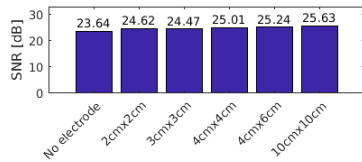


Figure 13. Changing the size of the ground electrode. The average $SNR = 24.77$ dB (with $SD=0.69$).

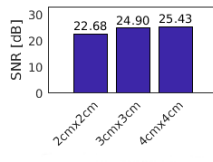


Figure 14. Changing the size of the signal electrode. The average $SNR = 24.34$ dB (with $SD=1.46$).

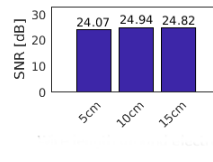


Figure 15. Changing the length of the wire towards the ground electrode. The average $SNR = 24.61$ dB (with $SD=0.47$).

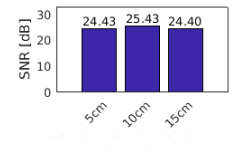


Figure 16. Changing the length of the wire towards the signal electrode. The average $SNR = 24.75$ dB (with $SD=0.59$).

As explained earlier, grounding is important in wearable BCC systems. To bring the devices to the common ground, BCC device designers try to push all devices' grounds towards the earth ground. This can be achieved by ensuring that the parasitic air-coupling between the device's ground and the earth ground is strong, which is usually done by dedicating a ground plate (electrode) in the circuit. Therefore, the size of the ground electrode is an important parameter. The TouchCom board dedicates the whole bottom layer of the PCB as ground plate (approx. $6 \times 7.6\text{cm}^2$), therefore it is not suitable for full exploration of the ground plate design space. As partial results, we still provide data on the changing external ground plate size, because it is not clear how much the bottom layer of the PCB – that itself could be exposed to EM-noise from other components of the PCB itself – can function as exclusive grounding solution. Figure 13 shows that by increasing the external ground plate size, the connection indeed is slightly stronger; but the system works well even without a dedicated electrode. However, the ground electrode is still crucial in future hardware/form factor designs, especially when the PCB size shrinks down.

While the ground electrode ensures coupling between the device's ground and the earth ground, the signal electrode exists to couple the electrical signal carrying the digital data to the user's body. Similar to the previous case, the capacitive coupling effect is stronger if the plate of the capacitor formed between the human and the device is larger. Therefore, by increasing the size of the signal electrode, we can increase the coupling to the user. Figure 14 confirms this tendency.

The electrodes (in other words: couplers) do not necessarily have to be an integral part of the BCC device. Figure 15 and Figure 16 show that placing them 5, 10, or 15 cms from the devices does not have a significant effect on performance. Going longer with the wires could increase the signal strength more noticeably³. Changing the material between the electrodes or the distance in between them does not seem to influence the signal strength (as long as non-conductive materials are used) (Figure 17 and Figure 18) – but once again, this can be a consequence of the TouchCom PCB design, and not necessarily a generalizable observation.

Location and Body Position

Several concepts and scenarios envision using BCC for human-centered connectivity of wearable devices. To understand the physical limitations of BCC, we evaluate various body

³As an extra measurement, once both the ground and signal electrode were connected by 1.2 m wires resulting in a significantly stronger signal ($SNR = 30.42$ dB compared to average $24.61 - 24.76$ dB).

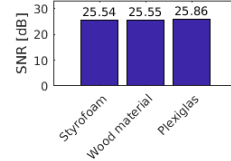


Figure 17. Changing the material between the signal and ground electrodes. The average $SNR = 25.65$ dB (with $SD=0.18$).

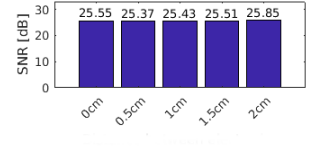


Figure 18. Changing the distance between the signal and ground electrodes. The average $SNR = 25.54$ dB (with $SD=0.19$).

locations. Moreover, each location is measured in several body positions. Figure 19 shows 16 RX locations (with a fixed TX position), in four different body positions: standing while the arms are wide spread; standing in a relaxed stance while the hand that wears the TX device touches the same side hip; sitting; and lying on the floor. For these types of measurements, the carrier frequency is configured to 4 MHz to reduce possible air-coupling (see section *Over-the-air Coupling*). This way we can better characterize the signal propagation throughout the body without accidentally "overhearing the signal" from other nearby body parts.

Whereas the second standing position (TX-hand on the hip) might seem as an unorthodox choice for a body configuration to be evaluated, it inherently differs from the standard standing position: touching the hip creates a shorter, direct (body) connection from the TX to the ground. In fact, that is the only position where the stomach and hip area can reach high signal levels, while at the same time, the signal strength noticeably drops at the generally good performing parts (the non-TX limbs).

Placing BCC devices on the wrist has been a popular option in the past, therefore this setup is evaluated in full details. However, some additional measurements are also performed to gain better understanding of the signal propagation when the TX is placed on the hip or on the feet (Figure 20 and 21). Observing the data from these inverse locations indicate that the placement of TX and RX pairs on the body (while both are located at limbs) is interchangeable regarding the signal strength: placing the TX on the wrist and the RX on the foot result in the same level of magnitude as placing the RX on the wrist and the TX on the foot. In case of the wrist-hip combination we can see a drop when the TX is placed on the hip. Most probably this comes from the hip generally being a poor location for either of the communication endpoint roles.

Overall, Figures 19-21 show that neither the TX-RX air-distance, nor the TX-RX distance measured on the body sur-

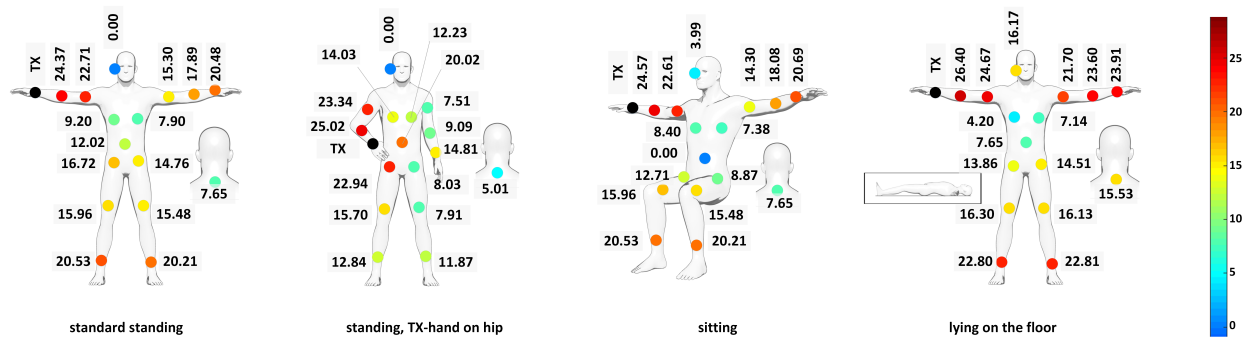


Figure 19. The signal strength varies across the body, and it is also affected by the position the user takes during transmission. Generally, limbs show high SNR values, while the chest and neck areas work poorly. The carrier frequency is set to 4 MHz.

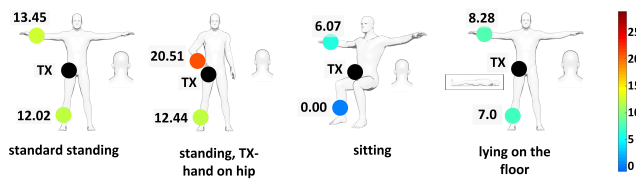


Figure 20. Signal strength measured at main locations while TX is located on the hip, in 4 different body positions. The carrier frequency is set to 4 MHz.

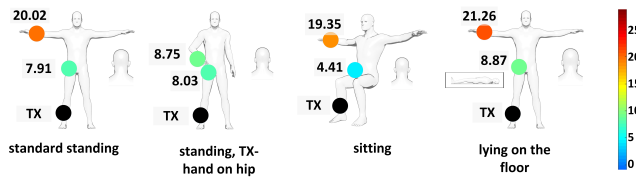


Figure 21. Signal strength measured at main locations while TX is located on the right foot, in 4 different body positions. The carrier frequency is set to 4 MHz.

face indicate what the strength of the signal is going to be. While in the frequency domain of TouchCom, the skin effect is prevalent (the EM-waves staying on the surface of the skin, opposed to flowing inside, through the body cells), it is not clear how much the underlying tissues actually influence the signal. Generally, the signal is the strongest on the limbs, but placing a device works reasonably well along the whole arms and legs (and hips as receivers). The neck, chest, and ears are weak locations.

Multiple Participants

Section *Location and Body Position* shows how different body positions can affect the signal propagation. To investigate this effect further, more complex body positions are evaluated by adding one more user to the setup. While the TX is still attached to the first person, the RX is placed on a second person. Figures 22-24 show three different relative body positions, each with four subconfigurations: each combination of TX and RX hand-placement is measured. The carrier frequency is set to 4 MHz, for the same reason as in Section *Location and Body Position*: to reduce possible over-the-air coupling between body parts.

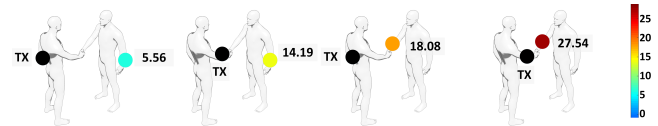


Figure 22. Signal strength measured on second person, during a handshake. All four combination of TX and RX wrist-placement is evaluated. The carrier frequency is set to 4 MHz.

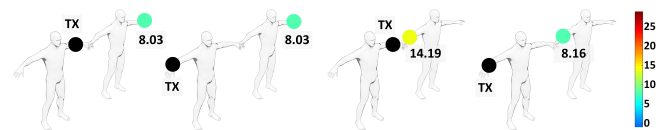


Figure 23. Signal strength measured on second person, while holding hands. All four combination of TX and RX wrist-placement is evaluated. The carrier frequency is set to 4 MHz.

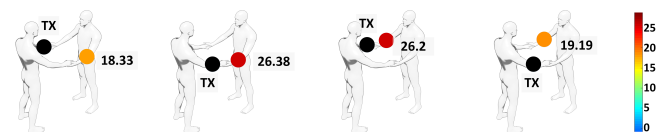


Figure 24. Signal strength measured on second person, while holding both hands. All four combination of TX and RX wrist-placement is evaluated. The carrier frequency is set to 4 MHz.

The results show that whenever two people are in contact and relatively close to each other, the signal is strong enough to propagate between them. However, when the length of the signal path increases, the signal strength drops. This is the most visible with the handshake while wearing the BCC wristbands on the relaxed hands (Figure 22.A). In addition, the side-by-side standing position also shows poor propagation (Figure 23.A, 23.B, and 23.D), except in the case when the TX-RX distance is extremely small (Figure 23.C).

Impact of Movements

Movements may disrupt the electric field around the user. Several different movement types are evaluated to understand the extent of this influence. Each movement is measured three times. To increase the recording window from 300 ms to 3 s, the ADC is reconfigured for these measurements. By decreasing the sampling rate, we loose precision, but the recording

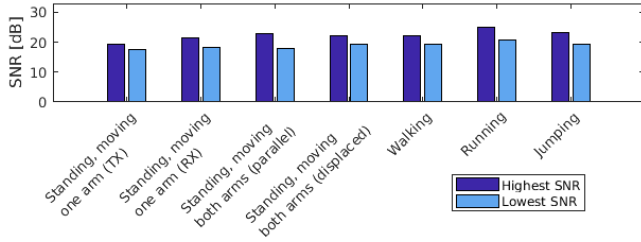


Figure 25. Changes in signal strength during movements, carried out in office environment. Walking, running, and jumping are performed while staying in one place. During walking and running the arms are hanging down, swinging to 30 degree angle. The strongest (highest SNR) and weakest (lowest SNR) values observed are plotted. The carrier frequency is set to 8 MHz.

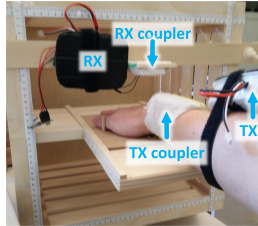


Figure 26. Wooden box to measure over-the-air coupling around the hands. While the TX is attached to the user, the RX can be freely moved around, covering a wide range of possible TX-RX distances and directions.

window can be prolonged. Figure 25 shows the changing signal throughout the observed movements. The maximum and minimum signal values are shown as maximum and minimum SNR. As expected, movements indeed have visible impact on the signal propagation, especially if the intensity of the movements increases. However, in most cases, the system still provides reliable performance during movements: the signal level never merged with the noise level during movements, and so a 0 bit could always be distinguished from a 1 bit.

Over-the-air Coupling

This paper investigates the type of BCC that uses EM-fields. Even though the body is used as the primary medium during these transmissions, some over-the-air coupling can still occur. A special measuring box is built to investigate the extent of over-the-air coupling around the two hands (Figure 26). A user wearing a TX can place his/her hand into the box, onto a wooden plate, while an RX can be attached to the box itself. The location of the RX can be changed to any distance and any direction from the wooden plate, therefore the signal can be easily measured in the 3D space around the hand. Figure 27 shows all the locations where the signal strength is measured. The distances shown are measured from the closest part of the hand. The box consists of exclusively non-metallic parts to avoid interfering with the electric field.

The results reported in Section *Reproducibility* already show that a higher frequency usually results in stronger signals. Figure 28 confirms that observation again. Additionally, the extent of over-the-air coupling is also stronger in case of the

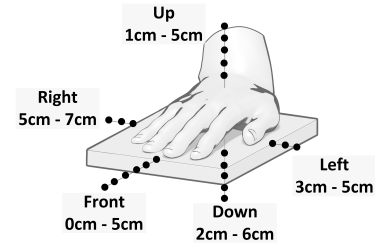


Figure 27. Locations to measure the signal over the air. The shown distances are measured from the closest part of the hand (skin).

higher frequency⁴. Moreover, over-the-air coupling is also stronger around the TX wearing compared to the *free* hand.

DISCUSSION

General remarks

Section *Reproducibility* confirmed that the prototype devices used during our measurements give reliable results over time, therefore we consider the results presented later comparable to each other. The section did not identify any major influencer coming from varying circumstances (different users, different environments, different clothing). The most notable finding of Section *Physical Design Parameters of BCC Devices* is that the electrodes can be separated from the device up to a distance. This might be beneficial for designs that involve electric textile clothing. Measurements considering the electrode size might be inconclusive since the used BCC prototype already had good grounding qualities. In contrast, the investigation of signal electrode size clearly shows that decreasing its size leads to weaker signals.

Interpreting signal-to-noise ratio values

Before analyzing the presented results and their implications from application design point of view, the connection between achievable network performance and the presented SNR values must be established. Therefore, we performed a controlled series of measurements using a directly connected TouchCom TX and RX pair. Using controllable gain for the TX output power it is possible to simulate differently distorted channel conditions. Figure 29 shows data rate and PER (packet error rate), derived from measurements taken during heavy data traffic between the devices (packets are sent every 10 ms). Figure 30 summarizes the relationship between SNR and network performance by establishing definitions for *excellent*, *good*, and *weak* signals. It is important to note that these numbers reflect on the current software implementation of TouchCom, and a more advanced implementation could result in better network performance in the future.

Application design: a BCC music streamer example

To demonstrate how to use the findings of this paper for the design process of a BCC application, we use the following example. The core idea is to use BCC for a novel music streaming application: by touching objects or people, or just

⁴Parasitic capacitances getting stronger at higher frequencies was an expected behavior since the capacitive reactance formula is frequency dependant ($X_C = 1/(2\pi fC)$).

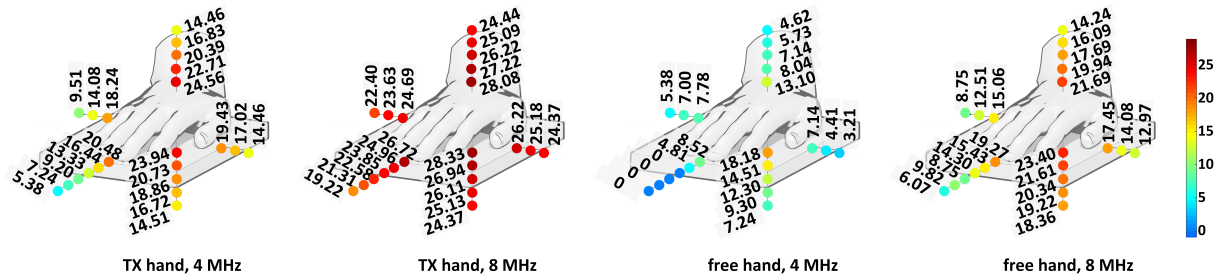


Figure 28. Over-the-air coupling measurements. The user has a TX on his left hand. Both hands are measured to analyze the extent of over-the-air coupling. The user is in standard standing position.

by carrying music storage devices, audio could be streamed to a pair of headphones.

As a general pointer, data collected during Section *Location and Body Position* can be used to understand the performance of different device placements on the body. In case of headphones, the results suggest weak performance around the user’s head. Therefore, streaming from a wristband using BCC to a headphone is probably difficult to implement. An exception could be a music streaming bed or couch: just by lying on the BCC bed, data could be reliably received by the BCC headphones.

Additionally, for generic data transfer and without constraining the application to specific body positions, necklaces and chest strap designs should be avoided as well, since they tend to have weak signals. Belts or pocket devices perform better, but they do not guarantee continuously strong signals (they change across different body positions). On the other hand, reliably stable performance can be expected on the limbs, favoring wristband or shoe-integrated designs.

Even if BCC cannot be used to stream audio between the storage device and the headphones, we could still use BCC for control, by extracting audio ID information from physical objects. By touching or standing on BCC objects, the users’ wristbands can gain information from the objects about which audio track to play. Afterwards, a backbone system can make sure that the headphone indeed receives the stream through a suitable communication channel.

Nevertheless, it is important to note that the data presented in Section *Location and Body Position* was measured with 4 MHz. Generally, it can be expected that by going higher with the frequency all presented values possibly get boosted – as Figures 6, 7, and 12 suggest. This signal strength boost, however, comes at the cost of significantly increasing *over-the-air coupling*, as seen in the relevant section. Overcoming this over-the-air coupling effect from the software is not trivial either: weak signals can always indicate hovering limbs as much as direct contact with *less conductive* body parts. Therefore, the decision if, e.g., amplitude thresholding is a suitable solution depends always on the desired use cases of the proposed application.

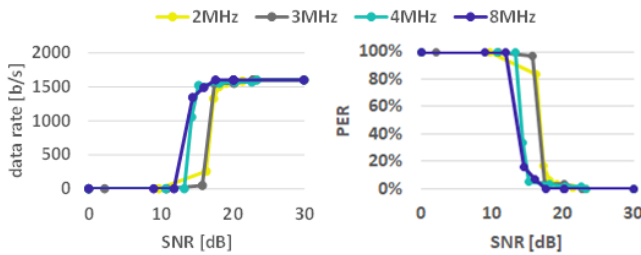


Figure 29. Data rate and PER (packet error rate) as a function of SNR. The system performs similarly across different carrier frequencies.

In our case, it may be possible to create the audio streaming BCC headphone using a higher carrier frequency (maybe even higher than 8 MHz) or higher output voltage on the transmitter (Figure 1.A). However, in this case the touch-trigger characteristic is lost. On 8 MHz, the signal is still very strong from 4-6 cm, and possibly detectable up to 10 cm. These observations imply that the music streaming application can either use touch for control but not for streaming itself (using 4 MHz or lower), or for streaming but not for control (using 8 MHz or higher).

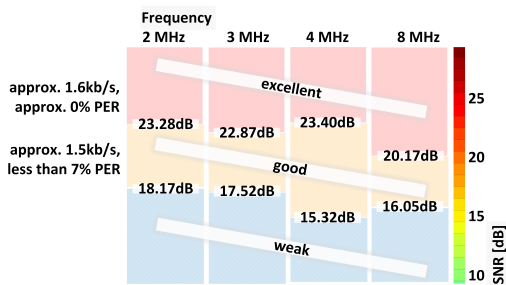


Figure 30. Relationship between SNR and achievable performance per frequency.

The BCC music streamer could also be a platform to share music between people. For example, while a person is streaming from her own BCC wristband to her BCC headphone, she could share the audio to another BCC headphone-wearing person just by holding their hands. Considering that Section *Multiple Participants* was measured at 4 MHz, we face a similar situation as above: to guarantee a robust connection independent of body position, we should go with a higher frequency. This choice, however, could lead to unintentionally *leak* the signal to other people who are just standing nearby.

Once again, the intended application context can dictate the parameter choice. By supplying BCC headphones to a group

of people on the dance floor, partners can share music between them while dancing. By choosing 4 MHz as carrier frequency we can ensure that each dancing couple can enjoy their own music (the signal strength is excellent while holding both hands), without interfering with others (over-the-air coupling is minimal). This application implements the silent disco⁵ concept with an addition of being able to customize the streamed music uniquely to each dancing couple. The partners' BCC wristbands can identify whom they dance with, and this information then can be forwarded to a backbone system that can choose music based on shared interest.

We discuss how movements influence the BCC stream in Section *Impact of Movements*. That data suggests that if the silent disco wanted to use BCC-streaming headphones (as opposed to BCC-controlled headphones), the 4 MHz signal might be disrupted: even the recorded 8 MHz signal shows a slight drop in signal strength during heavy movements (Figure 25). However, if BCC is used only for *pairing the couple* (understanding who is dancing with whom) to be able to select the right music for each couple, and the music streaming itself uses a separate channel (like WiFi), then the effects of movements can be omitted.

Other interactions and use cases

The earlier sections did not only provide quantified data on the channel characteristic of the human body during EM-field based data transmission, but they also revealed that BCC has the potential to be used in the context of a whole body user interface: not only the limbs can be part of the digital communication or interaction (as has been the focus of earlier work), but other body parts can be employed as well.

Therefore, the idea of streaming data from BCC smartwatches to BCC headphones can be generalized. On-body sensor networks can be created where different body-worn devices communicate throughout the body. Chest strap heart rate monitors can stream data towards the smartphone attached to the arms while running (Figure 1.B). Even though movements somewhat disrupt the BCC signal (as seen in Section *Impact of Movements*), using higher frequencies can keep the signal on the *good* level.

Seamless authentication of smart doors can also be implemented using BCC: a BCC unit waiting for the correct code can be attached to the door, with its signal electrode being connected to the door knob. If the right code is received through touching the knob, the BCC unit would open the lock mechanism, enabling opening the door without keys or cards. For this setup, the user could wear a BCC wristband holding his/her ID. Based on Section *Location and Body Position*, touching the knob with either hand would work. Furthermore, if the signal electrode of the door unit is extended to the whole door and not just the knob itself, then the user can use her/his

⁵“A silent disco is an event where people dance to music listened to on wireless headphones. Rather than using a speaker system, music is broadcast via a radio transmitter with the signal being picked up by wireless headphone receivers worn by the participants. Those without the headphones hear no music, giving the effect of a room full of people dancing to nothing.”[3]

elbow, hip, or feet as well to make contact with (and subsequently unlock) the door (Figure 1.C). False openings, without actually touching the knob should be minimized, which suggests to choose the carrier frequency around 4 MHz. However, going up with the frequency could increase the signal level so that *Multiple Participants* configurations could be explored: a child (without wearing a BCC device) could only open the door while its hand is being held by the key-owner parent (Figure 1.D).

ACKNOWLEDGMENTS

We thank Chris Harrison for providing feedback and guidance on this paper and Maurizio Nitti for creating the artwork. We appreciate the helpful comments from the reviewers of this and previous submissions. Furthermore, we thank all the volunteers who participated in the experiments.

CONCLUSION

While novel capacitively coupled interaction techniques keep emerging in the HCI community, modeling the exact behavior of the signal propagation in such systems is still an unsolved problem due to the number of parameters that may have an influence on the occurring electric fields. This paper focuses on a special class of capacitive wearables: Body Channel Communication (BCC) employs the human body to transfer data signals through it.

We present a comprehensive empirical study on the channel characteristics of BCC systems by covering major practical aspects that should be considered when designing wearable BCC devices and applications: reproducibility over time; behavior in different environments, with different users; physical design parameters of the transceiver devices; possible device placements (with detailed body location map) considering different body positions and movements; possibility of two-person networks; and touch sensitivity (as indicated by the strength of over-the-air signal propagation).

In addition to presenting the performance of the body channel under varied configurations, we continue the discussion with reflecting on the implications of this performance, and what they mean from an application designer's perspective. The described case study demonstrates how the quantified results can be interpreted in higher abstraction levels.

At last, we explore the novel interaction and connectivity opportunities that opened up after analyzing the results. We argue that BCC is a technology that can extend the traditional interpretation of user interfaces to the whole surface of body. Moreover, BCC can also recognize and utilize multi-people interactions.

BCC is a promising technology that allows designers to combine communication with physical interaction when touching the infrastructure or other people, or while simply wearing BCC-objects. Without doubt there will be future studies that provide additional information about the operation of such systems. We hope that the data presented here together with the discussion of the parameter space and their implications, provide designers of future BCC devices and applications a solid starting point to explore this exciting technology.

REFERENCES

1998. ICNIRP Guidelines for Limiting Exposure to Time-Varying Electric, Magnetic and Electromagnetic Fields (Up to 300 GHz). *HEALTH PHYSICS* 74 (1998), 494–522. Reconfirmed in 2009 until further notice: <https://www.ncbi.nlm.nih.gov/pubmed/19667809>.
2012. IEEE Standard for Local and metropolitan area networks - Part 15.6: Wireless Body Area Networks. *IEEE Std 802.15.6-2012* (2012).
2018. Wikipedia: Silent Disco. Website. (04 2018). https://en.wikipedia.org/wiki/Silent_disco.
- Joonsung Bae, Hyunwoo Cho, Kiseok Song, Hyungwoo Lee, and Hoi-Jun Yoo. 2012. The Signal Transmission Mechanism on the Surface of Human Body for Body Channel Communication. *Microwave Theory and Techniques, IEEE Transactions on* 60, 3 (March 2012), 582–593. DOI: <http://dx.doi.org/10.1109/TMTT.2011.2178857>
- Heribert Baldus, Steven Corroy, Alberto Fazzi, Karin Klabunde, and Tim Schenk. 2009. Human-Centric Connectivity Enabled by Body-Coupled Communications. *Communications Magazine, IEEE* 47, 6 (June 2009), 172–178. DOI: <http://dx.doi.org/10.1109/MCOM.2009.5116816>
- Gabe Cohn, Daniel Morris, Shwetak Patel, and Desney Tan. 2012. Humantenna: Using the Body As an Antenna for Real-time Whole-body Interaction. In *Proceedings of the SIGCHI Conference on Human Factors in Computing Systems (CHI '12)*. ACM, New York, NY, USA, 1901–1910. DOI: <http://dx.doi.org/10.1145/2207676.2208330>
- Paul Dietz and Darren Leigh. 2001. DiamondTouch: A Multi-user Touch Technology. In *Proceedings of the 14th Annual ACM Symposium on User Interface Software and Technology (UIST '01)*. ACM, New York, NY, USA, 219–226. DOI: <http://dx.doi.org/10.1145/502348.502389>
- David Dobbstein, Philipp Hock, and Enrico Rukzio. 2015. Belt: An Unobtrusive Touch Input Device for Head-worn Displays. In *Proceedings of the 33rd Annual ACM Conference on Human Factors in Computing Systems (CHI '15)*. ACM, New York, NY, USA, 2135–2138. DOI: <http://dx.doi.org/10.1145/2702123.2702450>
- Francine Gemperle, Chris Kasabach, John Stivoric, Malcolm Bauer, and Richard Martin. 1998. Design for wearability. In *Digest of Papers. Second International Symposium on Wearable Computers (Cat. No.98EX215)*. 116–122. DOI: <http://dx.doi.org/10.1109/ISWC.1998.729537>
- Tobias Grosse-Puppenthal, Sebastian Herber, Raphael Wimmer, Frank Englert, Sebastian Beck, Julian von Wilmsdorff, Reiner Wichert, and Arjan Kuijper. 2014. Capacitive Near-field Communication for Ubiquitous Interaction and Perception. In *Proceedings of the 2014 ACM International Joint Conference on Pervasive and Ubiquitous Computing (UbiComp '14)*. ACM, New York, NY, USA, 231–242. DOI: <http://dx.doi.org/10.1145/2632048.2632053>
- Tobias Grosse-Puppenthal, Christian Holz, Gabe Cohn, Raphael Wimmer, Oskar Bechtold, Steve Hodges, Matthew S. Reynolds, and Joshua R. Smith. 2017. Finding Common Ground: A Survey of Capacitive Sensing in Human-Computer Interaction. In *Proceedings of the 2017 CHI Conference on Human Factors in Computing Systems (CHI '17)*. ACM, New York, NY, USA, 3293–3315. DOI: <http://dx.doi.org/10.1145/3025453.3025808>
- Marian Haescher, Denys J. C. Matthies, Gerald Bieber, and Bodo Urban. 2015. CapWalk: A Capacitive Recognition of Walking-based Activities As a Wearable Assistive Technology. In *Proceedings of the 8th ACM International Conference on Pervasive Technologies Related to Assistive Environments (PETRA '15)*. ACM, New York, NY, USA, Article 35, 8 pages. DOI: <http://dx.doi.org/10.1145/2769493.2769500>
- Chris Harrison, Munehiko Sato, and Ivan Poupyrev. 2012. Capacitive Fingerprinting: Exploring User Differentiation by Sensing Electrical Properties of the Human Body. In *Proceedings of the 25th Annual ACM Symposium on User Interface Software and Technology (UIST '12)*. ACM, New York, NY, USA, 537–544. DOI: <http://dx.doi.org/10.1145/2380116.2380183>
- Mehrdad Hesar, Vikram Iyer, and Shyamnath Gollakota. 2016. Enabling On-body Transmissions with Commodity Devices. In *Proceedings of the 2016 ACM International Joint Conference on Pervasive and Ubiquitous Computing (UbiComp '16)*. ACM, New York, NY, USA, 1100–1111. DOI: <http://dx.doi.org/10.1145/2971648.2971682>
- Christian Holz, Senaka Buthpitiya, and Marius Knaust. 2015. Bodyprint: Biometric User Identification on Mobile Devices Using the Capacitive Touchscreen to Scan Body Parts. In *Proceedings of the 33rd Annual ACM Conference on Human Factors in Computing Systems (CHI '15)*. ACM, New York, NY, USA, 3011–3014. DOI: <http://dx.doi.org/10.1145/2702123.2702518>
- Christian Holz and Marius Knaust. 2015. Biometric Touch Sensing: Seamlessly Augmenting Each Touch with Continuous Authentication. In *Proceedings of the 28th Annual ACM Symposium on User Interface Software & Technology (UIST '15)*. ACM, New York, NY, USA, 303–312. DOI: <http://dx.doi.org/10.1145/2807442.2807458>
- Hsin-Liu (Cindy) Kao, Artem Dementyev, Joseph A. Paradiso, and Chris Schmandt. 2015. NailIO: Fingernails As an Input Surface. In *Proceedings of the 33rd Annual ACM Conference on Human Factors in Computing Systems (CHI '15)*. ACM, New York, NY, USA, 3015–3018. DOI: <http://dx.doi.org/10.1145/2702123.2702572>

18. Hsin-Liu (Cindy) Kao, Christian Holz, Asta Roseway, Andres Calvo, and Chris Schmandt. 2016. DuoSkin: Rapidly Prototyping On-skin User Interfaces Using Skin-friendly Materials. In *Proceedings of the 2016 ACM International Symposium on Wearable Computers (ISWC '16)*. ACM, New York, NY, USA, 16–23. DOI: <http://dx.doi.org/10.1145/2971763.2971777>
19. Muhammad Irfan Kazim. 2015. *Variation-Aware System Design Simulation Methodology for Capacitive BCC Transceivers*. Ph.D. Dissertation. Linköping University Electronic Press.
20. Gierad Laput, Chouchang Yang, Robert Xiao, Alanson Sample, and Chris Harrison. 2015. EM-Sense: Touch Recognition of Uninstrumented, Electrical and Electromechanical Objects. In *Proceedings of the 28th Annual ACM Symposium on User Interface Software & Technology (UIST '15)*. ACM, New York, NY, USA, 157–166. DOI: <http://dx.doi.org/10.1145/2807442.2807481>
21. Darren Leigh, Clifton Forlines, Ricardo Jota, Steven Sanders, and Daniel Wigdor. 2014. High Rate, Low-latency Multi-touch Sensing with Simultaneous Orthogonal Multiplexing. In *Proceedings of the 27th Annual ACM Symposium on User Interface Software and Technology (UIST '14)*. ACM, New York, NY, USA, 355–364. DOI: <http://dx.doi.org/10.1145/2642918.2647353>
22. Zeljka Lucev, Igor Krois, and Mario Cifrek. 2012a. A Capacitive Intrabody Communication Channel from 100 kHz to 100 MHz. *Instrumentation and Measurement, IEEE Transactions on* 61, 12 (Dec 2012), 3280–3289. DOI: <http://dx.doi.org/10.1109/TIM.2012.2205491>
23. Zeljka Lucev, Igor Krois, and Mario Cifrek. 2012b. Effect of Body Positions and Movements in a Capacitive Intrabody Communication Channel from 100 kHz to 100 MHz. In *Instrumentation and Measurement Technology Conference (I2MTC), IEEE International*. 2791–2795. DOI: <http://dx.doi.org/10.1109/I2MTC.2012.6229459>
24. Nobuyuki Matsushita, Shigeru Tajima, Yuji Ayatsuka, and Jun Rekimoto. 2000. Wearable Key: Device for Personalizing Nearby Environment. In *Wearable Computers, The Fourth International Symposium on*. 119–126. DOI: <http://dx.doi.org/10.1109/ISWC.2000.888473>
25. Nafiseh S. Mazloum. 2008. *Body-Coupled Communications - Experimental Characterization, Channel Modeling and Physical Layer Design*. Master's thesis. Chalmers University of Technology and Philips Research.
26. Kurt Partridge, Bradley Dahlquist, Alireza Veisheh, Annie Cain, Ann Foreman, Joseph Goldberg, and Gaetano Borriello. 2001. Empirical Measurements of Intrabody Communication Performance Under Varied Physical Configurations. In *Proceedings of the 14th Annual ACM Symposium on User Interface Software and Technology (UIST '01)*. ACM, New York, NY, USA, 183–190. DOI: <http://dx.doi.org/10.1145/502348.502381>
27. Ivan Poupyrev, Nan-Wei Gong, Shiho Fukuhara, Mustafa Emre Karagozler, Carsten Schwesig, and Karen E. Robinson. 2016. Project Jacquard: Interactive Digital Textiles at Scale. In *Proceedings of the 2016 CHI Conference on Human Factors in Computing Systems (CHI '16)*. ACM, New York, NY, USA, 4216–4227. DOI: <http://dx.doi.org/10.1145/2858036.2858176>
28. Ai-Ichiro Sasaki, Mitsuru Shinagawa, and Katsuyuki Ochiai. 2009. Principles and Demonstration of Intrabody Communication With a Sensitive Electrooptic Sensor. *Instrumentation and Measurement, IEEE Transactions on* 58, 2 (Feb 2009), 457–466. DOI: <http://dx.doi.org/10.1109/TIM.2008.2003307>
29. Munehiko Sato, Ivan Poupyrev, and Chris Harrison. 2012. Touché: Enhancing Touch Interaction on Humans, Screens, Liquids, and Everyday Objects. In *Proceedings of the SIGCHI Conference on Human Factors in Computing Systems (CHI '12)*. ACM, New York, NY, USA, 483–492. DOI: <http://dx.doi.org/10.1145/2207676.2207743>
30. Tim C. W. Schenk, Nafiseh S. Mazloum, Luc Tan, and Peter Rutten. 2008. Experimental Characterization of the Body-Coupled Communications Channel. In *Wireless Communication Systems (ISWCS), 2008. IEEE International Symposium on*. 234–239. DOI: <http://dx.doi.org/10.1109/ISWCS.2008.4726053>
31. MirHojjat Seyedi, Zibo Cai, and Daniel Lai. 2011. Characterization of Signal Propagation through Limb Joints for Intrabody Communication. *International Journal of Biomaterials Research and Engineering* 1(2) (2011), 1–12.
32. Gurashish Singh, Alexander Nelson, Ryan Robucci, Chintan Patel, and Nilanjan Banerjee. 2015. Inviz: Low-power personalized gesture recognition using wearable textile capacitive sensor arrays. In *2015 IEEE International Conference on Pervasive Computing and Communications (PerCom)*. 198–206. DOI: <http://dx.doi.org/10.1109/PERCOM.2015.7146529>
33. Virag Varga, Gergely Vakulya, Alanson Sample, and Thomas R. Gross. 2017. Playful Interactions with Body Channel Communication: Conquer It!. In *Adjunct Publication of the 30th Annual ACM Symposium on User Interface Software and Technology (UIST '17)*. ACM, New York, NY, USA, 81–82. DOI: <http://dx.doi.org/10.1145/3131785.3131798>
34. Virag Varga, Gergely Vakulya, Alanson Sample, and Thomas R. Gross. 2018. Enabling Interactive Infrastructure with Body Channel Communication. *Proc. ACM Interact. Mob. Wearable Ubiquitous Technol.* 1, 4, Article 169 (Jan. 2018), 29 pages. DOI: <http://dx.doi.org/10.1145/3161180>

35. Edward Jay Wang, Jake Garrison, Eric Whitmire, Mayank Goel, and Shwetak Patel. 2017. Carpacio: Repurposing Capacitive Sensors to Distinguish Driver and Passenger Touches on In-Vehicle Screens. In *Proceedings of the 30th Annual ACM Symposium on User Interface Software and Technology (UIST '17)*. ACM, New York, NY, USA, 49–55. DOI : <http://dx.doi.org/10.1145/3126594.3126623>
36. Martin Weigel, Tong Lu, Gilles Bailly, Antti Oulasvirta, Carmel Majidi, and Jürgen Steimle. 2015. iSkin: Flexible, Stretchable and Visually Customizable On-Body Touch Sensors for Mobile Computing. In *Proceedings of the 33rd Annual ACM Conference on Human Factors in Computing Systems (CHI '15)*. ACM, New York, NY, USA, 2991–3000. DOI : <http://dx.doi.org/10.1145/2702123.2702391>
37. Raphael Wimmer, Matthias Kranz, Boring Sebastian, and Albrecht Schmidt. 2007. A Capacitive Sensing Toolkit for Pervasive Activity Detection and Recognition. In *Fifth Annual IEEE International Conference on Pervasive Computing and Communications (PerCom'07)*. 171–180. DOI : <http://dx.doi.org/10.1109/PERCOM.2007.1>
38. Ruoyu Xu, Wai Chiu Ng, Hongjie Zhu, Hengying Shan, and Jie Yuan. 2012. Equation environment coupling and interference on the electric-field intrabody communication channel. *IEEE Transactions on biomedical engineering* 59, 7 (2012), 2051–2059.
39. Chouchang Jack Yang and Alanson P. Sample. 2017. EM-Comm: Touch-based Communication via Modulated Electromagnetic Emissions. *Proc. ACM Interact. Mob. Wearable Ubiquitous Technol.* 1, 3, Article 118 (Sept. 2017), 24 pages. DOI : <http://dx.doi.org/10.1145/3130984>
40. Dongwook Yoon, Ken Hinckley, Hrvoje Benko, François Guimbretière, Pourang Irani, Michel Pahud, and Marcel Gavrilu. 2015. Sensing Tablet Grasp + Micro-mobility for Active Reading. In *Proceedings of the 28th Annual ACM Symposium on User Interface Software & Technology (UIST '15)*. ACM, New York, NY, USA, 477–487. DOI : <http://dx.doi.org/10.1145/2807442.2807510>
41. Yang Zhang, Junhan Zhou, Gierad Laput, and Chris Harrison. 2016. SkinTrack: Using the Body As an Electrical Waveguide for Continuous Finger Tracking on the Skin. In *Proceedings of the 2016 CHI Conference on Human Factors in Computing Systems (CHI '16)*. ACM, New York, NY, USA, 1491–1503. DOI : <http://dx.doi.org/10.1145/2858036.2858082>
42. Thomas G. Zimmerman. 1996. Personal Area Networks: Near-field Intrabody Communication. *IBM Syst. J.* 35, 3-4 (Sept. 1996), 609–617. DOI : <http://dx.doi.org/10.1147/sj.353.0609>
43. Thomas G. Zimmerman, Joshua R. Smith, Joseph A. Paradiso, David Allport, and Neil Gershenfeld. 1995. Applying Electric Field Sensing to Human-computer Interfaces. In *Proceedings of the SIGCHI Conference on Human Factors in Computing Systems (CHI '95)*. ACM Press/Addison-Wesley Publishing Co., New York, NY, USA, 280–287. DOI : <http://dx.doi.org/10.1145/223904.223940>